1	Optical recording reveals topological distribution of functionally classified
2	colorectal afferent neurons in intact lumbosacral DRG
3	Tiantian Guo, Zichao Bian, Kyle Trocki, Longtu Chen, Guoan Zheng, Bin Feng*
4	Department of Biomedical Engineering, University of Connecticut, CT 06269
5	Abbreviated title: Optical recording on colorectal DRG
6	Manuscript length: 19 pages, 6 figures, 0 tables
7	Words: 244 for Abstract, 688 for Introduction, 1942 for Discussion
8	<u>Conflict of interest</u> : The authors claim no conflict of interests.
9	Acknowledgements: supported by NIH K01DK100460 (BF), NIH R03DK114546
10	(BF), NSF CMMI-1727185 (BF), NIH R03EB022144 (GZ)
11	
12	
13	*Correspondence:
14	Bin Feng, Ph.D.
15	Department of Biomedical Engineering, University of Connecticut
16	260 Glenbrook Road, Unit 3247, Storrs, CT 06269-3247, USA
17	E-mail: fengb@uconn.edu
18	Phone: 860-486-6435, fax: 860-486-2500
19	

ABSTRACT

20

21

22

23

24

25

26

27

28

29

30

31

32

33

34

35

36

37

38

39

40

41

42

43

44

45

46

47

Neuromodulation as a non-drug alternative for managing visceral pain in irritable bowel syndrome (IBS) may target sensitized afferents of distal colon and rectum (colorectum), especially their somata in the dorsal root ganglion (DRG). Developing selective DRG stimulation to manage visceral pain requires knowledge of the topological distribution of colorectal afferent somata which are sparsely distributed in the DRG. Here, we implemented GCaMP6f to conduct high-throughput optical recordings of colorectal afferent activities in lumbosacral DRG, i.e., optical electrophysiology. Using a mouse ex vivo preparation with distal colorectum and L5-S1 DRG in continuity, we recorded 791 colorectal afferents' responses to graded colorectal distension (15, 30, 40, 60 mmHg) and/or luminal shear flow (20-30 mL/min), then functionally classified them into four mechanosensitive classes, and determined the topological distribution of their somata in the DRG. Of the 791 colorectal afferents, 90.8% were in the L6 DRG, 8.3% in the S1 DRG, and only 0.9% in the L5 DRG. L6 afferents had all 4 classes: 29% mucosal, 18.4% muscular-mucosal, 34% low-threshold (LT) muscular and 18.2% high-threshold (HT) muscular afferents. S1 afferents only had 3 classes: 19.7% mucosal, 34.8% LT muscular and 45.5% HT muscular afferents. All seven L5 afferents were HT muscular. In L6 DRG, somata of HT muscular afferents were clustered in the caudal region whereas somata of the other classes did not cluster in specific regions. Outcomes of this study can directly inform the design and improvement of next-generation neuromodulation devices that target the DRG to alleviate visceral pain in IBS patients.

SIGNIFICANCES

By establishing a novel optical approach to determine neural activities with single-spike resolution via GCaMP6f, the current study characterizes the neural encoding from hundreds of colorectal afferents (~800) in the DRG, which are sparse distributed and difficult to be recorded with conventional methods. High-threshold muscular afferents, i.e., putative colorectal nociceptors are clustered in the caudal

- region of the L6 DRG, which informs the spatially selective neuromodulation of colorectal nociceptors for better management of visceral pain.
- 50

51

KEYWORDS:

- GCaMP, calcium imaging, colon, electrophysiology, single-unit
- 53

INTRODUCTION

Patients with irritable bowel syndrome (IBS) typically exhibit reduced response thresholds to rectal distension, pain during normal bowel function, and increased tenderness and size in areas of somatic referral (i.e., hypersensitivity) (7, 19). The underlying mechanism(s) of this hypersensitivity is widely attributed to the impaired function of the brain-gut axis, particularly afferent sensitization, which appears necessary for the persistence of IBS-related pain and hypersensitivity (54, 55). Studies by us and others document the innervation of distal colorectum by four classes of mechanosensitive afferent fibers that are tuned to encode normal colorectal distension, mucosal shear stress, and/or high-intensity mechanical probing (3, 14-16, 20, 21, 37). Pharmacological approach for managing visceral pain by reversing peripheral afferent sensitization has limited success largely due to the off-target side effects (7). In contrast, peripheral neuromodulation significantly limits the off-target effects by focal delivery of physical energy to peripheral nerves (5), nerve roots (24, 57) and dorsal root ganglion (DRG) (34, 39). Thus, neuromodulation that targets sensitized colorectal afferents, especially their somata in the DRG has the potential as a non-drug alternative for managing visceral pain.

Colorectal afferent somata in mouse DRG have been labeled by neural tracing studies revealing that mouse distal colorectum is innervated by T13-L1 thoracolumbar and L5-S1 lumbosacral DRG (11), of which the lumbosacral innervation appears necessary for encoding and transmitting visceral nociception (35). In lumbosacral innervation, mouse colorectal neurons are concentrated in the L6 DRG, and are sporadic in the adjacent L5 and S1 DRG (11). Even in L6 DRG, colorectal neurons are the minorities contributing to <10% total DRG neurons, and appear to sparsely spread throughout the DRG without clustering in specific regions (36, 38). The vast majority of colorectal DRG neurons are small and medium in diameter, immunohistologically positive for TRPV1, CGRP, and NaV1.8 (1, 2, 10, 41). Unlike the cutaneous DRG neurons that can be distinctly divided into peptidergic (positive for calcitonin gene-related peptide [CGRP]) and non-peptidergic (positive for isolectin B4 [IB4])

populations (31, 52), a significant proportion of colorectal neurons are positive for both CGPR and IB4 (36). A recent mRNA sequencing study has further divided colorectal neurons into seven categories based upon their messenger RNA profiles (30).

83

84

85

86

87

88

89

90

91

92

93

94

95

96

97

98

99

100

101

102

103

104

105

106

107

108

109

110

111

112

Despite the aforementioned body of literature regarding the anatomy, molecular profiles, and neural encoding functions of colorectal afferents, further advancement of DRG neuromodulation for managing visceral pain requires knowledge on the topological distributions of functionally classified colorectal neurons in the DRG, which has not been investigated by prior studies. For instance, knowing the spatial location of high-threshold colorectal afferents (putative nociceptors) in specific lumbosacral DRG will likely inform the design of DRG stimulation to selectively target colorectal nociceptors while sparing other sensory afferents that may play important physiological roles for the pelvic floor organs. Determining the topological distribution of colorectal DRG neurons requires functional recordings from intact ganglion, which is challenged by the small proportion and sparse distribution of colorectal neurons in the DRG, and has been achieved by only a handful of studies via intracellular recordings by using a sharp quartz glass electrode (29, 40). However, this approach is technically challenging and cannot efficiently record a large number of neurons to reveal the topological distributions of the colorectal neurons. On the other hand, the GCaMP6f, one of the recent genetically encoded calcium indicators allows recording of intracellular Ca²⁺ transients that correlate with individual neural action potentials (8), allowing 'functional' characterization of those neurons via imaging their fluorescent GCaMP6f signals (9).

In this study, we developed an optical recording approach to characterize colorectal afferent functions in a mouse *ex vivo* preparation with distal colorectum, pelvic nerve, L5-S1 DRG and dorsal roots in continuity. We conducted fast imaging recordings (100 frames per second) of intracellular GCaMP6f signals in intact DRG to resolve the fast calcium transients in individual DRG somata, allowing functional characterization of colorectal DRG neurons using this imaging method, i.e., optical recording. By this high throughput approach, we determined the responses of 791 neurons to mechanical colorectal distension and/or mucosal shear stress, functionally

divided them into four classes, and identified their topological distributions in the lumbosacral DRG. Portions of these data have been reported in abstract form (23).

MATERIALS AND METHODS

All experiments were reviewed and approved by the University of Connecticut Institutional Animal Care and Use Committee.

Transgenic mice

The Ai95 mice (C57BL/6 background) carrying heterozygous GCaMP6f gene (strain# 28865, The Jackson Laboratory, CT) and homozygous VGLUT2-Cre mice (strain# 28863, Jackson Laboratory, CT) were crossbred. The Ai95 mice carried the gene "CAG-GCaMP6f" in the Gt(ROSA)26Sor locus, which was preceded by a LoxP-flanked STOP cassette to prevent its expression. By crossing Ai95 mice with VGLUT2-Cre mice, the Cre-expressing cell population has the STOP cassette trimmed, resulting in expression of GCaMP6f in glutamatergic neurons expressing type 2 vesicular glutamate transporter (VGLUT2), which made up the vast majority of sensory neurons innervating distal colon and rectum (colorectum) (4). Offspring of both sexes aged 8-14 weeks with both heterozygous GCaMP6f and VGLUT2-Cre genes (i.e., VGLUT2/GCaMP6f) were used for optical electrophysiological recordings.

To characterize the efficiency of VGLUT2-Cre mice in driving the expression in colorectal sensory neurons, we crossed the VGLUT2-Cre mice with a tdTomato reporter line (Ai14, strain#7914, The Jackson Laboratory, CT). Offspring with both heterozygous tdTomato (tdT) and VGLUT2-Cre genes, i.e., VGLUT2/tdT mice were used for anatomical tracing studies.

Anatomic tracing of colorectal DRG neurons

All surgeries were aseptic; anesthesia was initiated and maintained with 4% and 2% isoflurane inhalation, respectively. In VGLUT2/tdT mice, primary afferent neurons innervating the colorectum were identified in DRG tissue sections by the content of the fluorescent retrograde tracer fast blue (FB; #NC0182483, Fisher Scientific, East Greenwich, RI). FB tracer injection was performed 7 - 28 days prior to harvesting DRG. Mice were anesthetized with isoflurane, the distal colon was exposed by

laparotomy, and the colon wall was injected with FB (1 mg/100 μ l in sterile saline; 10 μ l total distributed into 2-4 sites) by a syringe with a 33 gauge needle (model 7643-01, Hamilton Company, Arlington, MA). Any leakage from injection sites was removed using a cotton-tipped applicator and the peritoneal cavity was rinsed with sterile saline before suturing muscle and skin separately. To alleviate pain and distress, meloxicam (2 mg/kg, Boehringer Ingelheim Vetmedica, Duluth, Georgia) was given three times in 72 hours for postoperative analgesia.

Immunohistochemistry

As previously described (21), VGLUT2/tdT mice were euthanized via CO₂ inhalation. The lumbosacral (L6-S1) DRG were harvested and fixed with 4% paraformaldehyde in 0.16 M phosphate buffer containing 14% picric acid (Sigma-Aldrich). After cryoprotection in 20% sucrose, fixed tissue was embedded in OCT compound (Sakura Finetek, Tokyo, Japan), frozen, and sectioned at 10 μm. Tissue sections were incubated with a rabbit antibody against the red fluorescent protein (1:1000, Rockland, Limerick, PA) and the signals were further amplified by Alexa Fluor® 594-conjugated anti-rabbit IgG (1:200, Abcam, Cambridge, MA).

Fast Blue-containing and immunostained DRG neurons were identified and quantified as detailed previously (36). Briefly, the 8-bit grayscale immune-images were set with a threshold that excluded at least 99.99% of background intensity based on its Gaussian distribution using ImageJ (version 1.8.0; NIH). The threshold value was calculated from the standard normal distribution (Z) equation: threshold = 3.72 SD + m, where 3.72 was the Z-score at P = 0.9999, SD and m were the Standard Deviation and mean of background intensities in 8-bit grayscale (0-255), respectively.

Ex vivo preparation of colorectum-pelvic nerve-DRG

Mice of the correct genotype 8-14 weeks of age were deeply anesthetized by intraperitoneal and intramuscular injection of a 0.4 mL cocktail of ketamine (120 mg/kg) and xylazine (10 mg/kg). Mice were then euthanized by perfusion from the left ventricle with modified ice-cold Krebs solution replacing sodium chloride with equal molar of sucrose (in mM: 236 Sucrose, 4.7 KCl, 25 NaHCO₃, 1.3 NaH₂PO₄, 1.2 MgSO₄.7H₂O, 2.5 CaCl₂, 11.1 D-Glucose, 2 butyrate, 20 acetate, 0.004 nifedipine and

0.003 indomethacin) bubbled with carbogen (95% O₂, 5% CO₂). A dorsal laminectomy was performed to expose the thoracic and lumbar spinal cord. The colorectum with attached S1, L6 and L5 spinal nerve and DRG was carefully dissected via blunt dissection, and transferred to a tissue chamber superfused with 32-34 °C Krebs solution (in mM: 117.9 NaCl, 4.7 KCl, 25 NaHCO₃, 1.3 NaH₂PO₄, 1.2 MgSO₄·7H₂O, 2.5 CaCl₂, 11.1 D-Glucose, 2 butyrate, 20 acetate, 0.004 nifedipine and 0.003 indomethacin) bubbled with carbogen (95% O₂, 5% CO₂), consistent with our prior ex vivo studies on colorectal afferents (15, 17). The colorectum was cannulated and connected to a custom-built distending device consisting of computer-controlled fluid valves and hydrostatic pressure columns of 15, 30, 45, and 60 mmHg filled with phosphate buffered saline (PBS).

Optical recording of evoked fluorescent GCaMP6f signal

We employed an upright microscope platform (BX51WI, Olympus, Waltham, MA) to capture one whole DRG with a water immersion 10x objective (UMPLFLN 10XW, 0.3 NA) using a regular halogen epi-illumination light source and a regular filter cube for sample illumination. A high-speed ultra-low noise sCMOS camera (Xyla-4.2P, 82% quantum efficiency, Andor Technology, South Windsor, CT) was used to capture high-resolution images (1920x1920, 2x2 bin) at 100 frames per second, which provided a spatial resolution of 1.6 pixels / µm sufficient to resolve individual DRG neurons. This system allowed the recording of Ca²⁺ transients to resolve individual action potentials (APs) in multiple GCaMP6f-expressing DRG neurons simultaneously.

We implemented an image analysis algorithm to automatically locate activated DRG neurons that had evoked APs (i.e., Ca²⁺ transients) based on intensity fluctuation across different frames. We performed marker-based watershed segmentation to label different cells (56), allowing automated recording of GCaMP6f Ca²⁺ signals in multiple DRG neurons. We integrated the image analysis algorithm into a plug-in program to work with Micro-Manager, an open-source microscopy software sponsored by the NIH (12). By using this image recording approach, colorectal DRG neurons were functionally characterized in intact L5 - S1 DRG at high

efficiency.

Validation of GCaMP transients as individual action potentials

To validate that image recordings of GCaMP transients correlated with individual APs, we conducted concurrent recordings of GCaMP signals and intracellular electrical potentials in intact DRG attached with dorsal roots. Action potentials were evoked by electrical stimulation of the dorsal root with a suction electrode (1 mA monopolar cathodic, 0.1 ms duration @ 0.5-4 Hz). In addition to the optical recording of GCaMP6f signal, DRG neurons with positive GCaMP6f response were individually impaled with a high impedance (100-300 M Ω) quartz electrode filled with 1.0 M potassium acetate for intracellular recordings of the cell potential by a patch-clamp amplifier (Multiclamp 700A, Molecular Devices, San Jose, CA). The APs were digitized at 20 kHz and stored by a Power 1401 interface (Cambridge Electronic Design), which was also programmed to trigger the GCaMP6f image recordings to ensure proper alignment of action potentials with GCaMP6f imaging data.

Afferent identification and classification

Mouse colorectal afferents were activated by two physiologically-correlated stimuli at the colorectum: stepped luminal distension by hydrostatic fluid column of phosphate buffered saline (PBS, 15, 30, 45, and 60 mmHg of 5-sec steps) and luminal shear flow of PBS (20-30 mL/min). Based upon response profiles to graded distension and luminal shear, colorectal DRG were functionally classified into 4 classes: low-threshold (LT) muscular, high-threshold (HT) muscular, mucosal, and muscular-mucosal classes. LT-muscular afferents responded to all four distension pressure levels whereas HT-muscular only responded to noxious distension pressure (30, 45 and 60 mmHg); colorectal intraluminal pressure beyond 20 mmHg was considered noxious to mice (14, 32). Mucosal afferents did not respond to distension but responded to luminal shear flow. Muscular-mucosal afferents responded to both luminal shear flow and colorectal distension at all four pressure levels.

Data recording and analysis

Extracted GCaMP6f signals in the form of pixel intensity (0-255) from individual

DRG neurons were normalized by the pre-stimulus intensity. Peak GCaMP6f transients were determined when the signal increased by 3% within 200 mSec. Proportions of afferent classes were compared by Chi-square test using SigmaPlot v11.0 (Systat software, Inc., San Jose, CA). P < 0.05 was considered significant.

RESULTS

In 3 male and 3 female VGLUT2/tdTomato mice, the colorectal neurons in the lumbosacral DRG (L5 to S1) were labeled by the neural tracer fast blue (FB) as shown in Fig. 1. Among the 87 FB-positive colorectal neurons (white arrows or arrowheads in Fig. 1), 78% (68/87) showed positive immunoreactivity to tdTomato as indicated by the white arrows in Fig. 1. The portions of tdTomato-positive neurons from male (36/47) and female mice (32/40) were comparable and thus neurons from both sexes were pooled together. This confirms the previous finding that the majority of colorectal DRG neurons express VGLUT2 and the VGLUT2-Cre efficiently drives the gene expression in lumbosacral colorectal afferents (4). Immunostaining results also show that only 68 out of 2060 (3.3%) tdTomato-positive DRG neurons from 15 DRG (L5 to S1) are FB-positive colorectal neurons, which confirms that the colorectal neurons are sparsely distributed in lumbosacral DRG.

As illustrated in Fig. 2A, GCaMP6f image recording and intracellular sharp electrode recording were conducted concurrently to assess whether GCaMP6f signals correlate with neural activities. Optical recordings were conducted at multiple focal planes 50 µm apart to ensure the capture of GCaMP6f signals throughout the contour of the DRG in the dorsal lateral view. As shown in Fig. 2B, the GCaMP6f transients closely correlate with individual action potentials evoked by 1 Hz electrical stimulation at the dorsal root. Stimulation was assessed at higher frequencies as shown in Fig. 2C, and the GCaMP6f signal is capable to resolve individual action potential spikes at up to 4 Hz as shown in Fig. 2D1. As shown in Fig. 2D2, the individual spikes cannot be reliably detected at a stimulus frequency of 8 Hz, but the elevated magnitude of the fluorescent signal provides a qualitative estimation of the afferent firing frequency (compare the 4 Hz and 8 Hz signals in Fig. 2C).

Fig. 3A illustrates an ex vivo colorectum-pelvic nerve-DRG preparation, in which afferent endings in the colorectum were subjected to two computer-controlled mechanical stimuli: graded colorectal distension by hydrostatic pressure (15 to 60 mmHg) and luminal shear flow (20-30 mL/min). As shown in Fig. 3B, colorectal

afferents' responses to graded colorectal distension were captured by GCaMP6f signals from individual DRG neurons. Distending pressure beyond 25 mmHg was considered noxious (14), and afferents with response threshold below and above 25 mmHg were categorized as low-threshold (LT) and high-threshold (HT), respectively. Displayed in Fig. 3C is a typical colorectal afferent response to luminal shearing flow, which is equivalent to fine stroking of the mucosal surface in prior studies (15, 16).

For either colorectal distension or luminal shearing flow tests, GCaMP6f images were continuously recorded for 27 sec at 100 frames/sec, generating a sequence of 2700 images. Fig 4 illustrates the custom-built plug-in software to Micro-Manager (12) that automatically extracts GCaMP6f transients from activated DRG neurons in those image sequences. After automatic detection of the neural boundaries by marker-based watershed segmentation in Fig. 4A, activated neurons with intensity fluctuation beyond the detection threshold were automatically labeled for extraction of GCaMP6f transients in Fig. 4B. Figure 4C shows the fluorescence intensity signals from the labeled regions in Fig. 4B.

As shown in Fig. 5, a total of 791 lumbosacral DRG neurons from 8 male and 6 female VGLUT2/GCaMP6f mice presented evoked GCaMP6f responses to either colorectal distension or luminal shear flow, of which the vast majority (90.7%) were in L6 DRG and the rest in S1 DRG. Only 8.3% colorectal afferent neurons were in the S1 DRG and almost no neurons were recorded in L5 DRG (0.9%, 7/791). Based upon the response profiles to low- or high-threshold (LT- or HT-) distension and luminal shearing, the colorectal afferents were divided into four classes: LT-muscular, HT-muscular, mucosal and muscular-mucosal. All four afferent groups were present in the L6 DRG whereas muscular-mucosal afferents were absent in the S1 DRG. The 7 L5 afferents were all HT-muscular. Among the 791 neurons, 472 were from male mice and 319 from female mice. There was no difference between males and females in either the DRG segment distributions (92% vs. 91% in L6, 8% vs. 9% in S1, p = 0.60) or the proportions of the four afferent classes (28% vs. 31% LT-muscular, 21% vs. 17% HT-muscular, 31% vs. 33% mucosal, 21% vs. 19% muscular-mucosal, p = 0.48). Thus, characterized neurons from both sexes were pooled together and displayed as

pie charts in Fig. 5. For the following topological study, neurons from both sexes were also pooled together.

The large number of characterized L6 DRG neurons (718) permits a topological analysis of colorectal afferents in the L6 DRG. As shown in Fig. 6A, GCaMP6f recordings were conducted on the dorsal lateral view of the L6 DRG, which was evenly divided into 60 grids to assess the topological distributions of the four colorectal afferents classes in Fig. 6B. Distribution of mucosal, LT-muscular and muscular-mucosal afferents are widespread in the L6 DRG. In contrast, HT-muscular afferents are clustered towards the caudal portion of the L6 DRG (Fig. 6B).

DISCUSSION

296

297

298

299

300

301

302

303

304

305

306

307

308

309

310

311

312

313

314

315

316

317

318

319

320

321

322

323

324

In this study, we implemented a new optical approach to functionally characterize hundreds of colorectal afferent neurons and determined their topological distributions in the lumbosacral DRG in an ex vivo preparation with colorectum, pelvic nerve, and DRG in continuity. Using GCaMP6f, an ultrasensitive and rapid genetically encoded calcium indicator, we show that DRG neural activities can be recorded at a resolution of individual action potentials with a regular upright fluorescent microscope and a high-speed ultra-low noise sCMOS camera. The use of a water immersion 10x objective with high numerical aperture ensures that the whole DRG can be captured in the field of view at an ultra-high frame rate (100 frames/sec), and monitoring neural activities from 600 to 2000 neurons in one DRG simultaneously. The frame rates of recording in previous studies are generally below 14 frames per second. Using similar calcium indicators (e.g., GCaMP3 or GCaMP6s), functional characterization of cutaneous sensory neural activities has been done previously (9, 13, 33, 50), but the long recovery time (over seconds) of those calcium indicators challenges the interpretation of consecutive action potential spikes from the GCaMP transients. The calcium indicator GCaMP6f with faster recovery time has been used by a recent study to characterize sensory afferents innervating the facial skin, which shows great potential for resolving individual action potentials (26).

To the best of our knowledge, this is the first study that utilizes GCaMP6f to

functionally characterize afferents innervating the viscera. From our prior single-fiber recording of pelvic nerves (14, 16-18, 20, 21, 37, 53), the firing rate of colorectal afferents at threshold input stimuli is much lower than many somatic counterparts, generating only a few action potential spikes to the stimulus of seconds-long duration. Thus, in order to characterize visceral afferents, recording individual action potentials in somata with high temporal resolution is required. This justifies the use of GCaMP6f which, compared to previous generations of GCaMPs, offers ultra-sensitivity to individual action potentials and rapid recovery time from fluorescent state. We implemented a high image recording rate (100 frames/sec) in our GCaMP6f recordings, which was sufficient to resolve consecutive action potentials. We used electrical stimulation at the attached dorsal root to activate DRG neurons in a predictable and reproducible manner. The close correlation of GCaMP6f transients with individual action potentials was validated by our concurrent optical and electrophysiological recordings from the same DRG neuron (Fig. 1). Using this approach, we confirm the robustness of the evoked GCaMP6f transients by individual action potentials, usually more than 3% of the baseline fluorescent level for an easy post-hoc data extraction. In our study, GCaMP6f fluorescence usually returns to the baseline level within 1 to 2 secs in the DRG somata. At stimulation frequencies above 0.5 Hz, temporal summation of the GCaMP6f transients starts to occur with a gradual increase in the baseline fluorescent level. Nonetheless, individual GCaMP6f transients can be resolved up to 4 Hz stimulation. At frequency beyond 4Hz, the accumulated fluorescence intensity can still serve as a proxy for the rate of action potential firing. However, across different DRG neurons, the magnitude of calcium transients evoked by the same level of neural activities can vary significantly, presumably reflecting variation in expression levels of GCaMP6f as well as different calcium storage and buffering (25). Thus, the use of the temporal spikes (i.e., the GCaMP transients) rather than the fluorescent GCaMP magnitude in this study provides a more robust functional characterization and classification of colorectal afferents.

325

326

327

328

329

330

331

332

333

334

335

336

337

338

339

340

341

342

343

344

345

346

347

348

349

350

351

352

353

354

This is also the first study to functionally characterize a large number, i.e.,

hundreds of colorectal neurons in intact DRG, which are the minorities in lumbosacral DRG making up less than 10% of total DRG neurons even in the most abundant L6 segment (11). Prior functional characterization of colorectal afferents relied on blind poking of the DRG with a sharp glass electrode, a low yield approach implemented only by a handful of studies. Malin et al. conducted intracellular recordings from DRG somata in a similar ex vivo preparation with colorectum, pelvic nerve and L6 DRG in continuity using a sharp glass electrode, revealing the low-threshold and high-threshold populations of neurons to graded colorectal distension (41). Hibberd et al. used a similar ex vivo approach and conducted recordings from a CGRP-Cre mouse line, documenting that 78% of colorectal neurons are positive for CGRP (29). Neither studies are able to record more than 100 colorectal DRG neurons, insufficient for a topological distribution study. In contrast, our current optical recording approach allows the neural activities to be recorded from one whole DRG when reproducible mechanical stimuli are applied to the attached colorectum. The use of an objective with relatively low magnification (10X) allows a longer depth of field to capture the fluorescent signals 40-70 µm below the DRG surface. We also moved the focal plane at 50 µm to capture all the DRG in the dorsal lateral view, by which 40-60% of the DRG regions could be monitored concurrently, similar to other optical recordings from lumbar DRG (9) and trigeminal ganglion (26). Given that 3.3% VGLUT2-positive neurons innervate the colorectum from our fast-blue tracing study, the fact that 20 -80 colorectal neurons are recorded in each DRG strongly indicates that the GCaMP6f recording can monitor the responses of 600 – 2400 neurons in the DRG. Also, our GCaMP6f approach in detecting individual action potentials is also robust and reliable with more than 3% change of the baseline fluorescent level following each action potential, in contrast to less than 1% fluorescent changes in optical recordings using voltage-sensitive dyes (6). Collectively by using the GCaMP6f and a 10x objective, we managed to characterize 791 lumbar colorectal neurons in 14 VGLUT2/GCaMP6f mice, a dramatic improvement in efficiency compared to the previous approach with sharp electrode recordings.

355

356

357

358

359

360

361

362

363

364

365

366

367

368

369

370

371

372

373

374

375

376

377

378

379

380

381

382

383

384

In this study, the colorectum was kept in the tubular shape and subjected to two

distinct mechanical stimuli for functional afferent characterization; graded luminal distension from non-noxious (<25 mmHg) to noxious range (>25 mmHg) and luminal shear flow (20-30 mL/min). This is different from the prior approach by us and others with colorectum cut open along the mesentery and pinned flat for easy access to afferent receptive fields (3, 15, 17, 22, 59). Single-fiber recordings from teased pelvic nerve filaments are less affected by the slight movement and perturbation of nerve fibers from the manual manipulations of the receptive fields in the flattened colorectum, e.g., von Frey probing, mucosal stroking, and circumferential stretch. However, optical recordings of GCaMP6f transients require the translational movement of the DRG to be no more than a few microns, a fraction of the DRG neural diameter. To achieve that, we removed the human manipulation by developing computer-controlled valve systems for applying the graded colorectal distension and luminal shear stimuli, which was qualitatively equivalent to the circumferential stretch and mucosal stroking in the previous stimuli (16). The proportion of muscular, mucosal and muscular-mucosal afferents identified in the current study generally agrees with the previous studies of flattened colorectum (15, 20, 21, 37), except that the mucosal and muscular-mucosal proportions are slightly smaller, likely reflecting the weaker stimulus of luminal shear flow than the 10mg mucosal stroking. The serosal afferents activated by punctate probing of the receptive field beyond the physiological stress range (14) are likely not characterized by the current stimuli. However, the term "serosal" appears to be a misnomer(19) as a recent study shows that almost no nerve endings are located in the colorectal serosa (51). Keeping the colorectum in tubular shape prevents the characterization of mechanically-insensitive afferents (MIAs), which were previously identified and characterized by us with focal electrical stimulation to the receptive fields in the flattened colorectum (15, 17). A recent study indicates those MIAs appear to express nicotinic acetylcholine receptor subunit alpha 3 (Chrna3) (47). Future studies could focus on the MIAs by selective expression of GCaMP6f in those Chrna3-positive DRG neurons. The high-threshold (HT) muscular afferents that encode noxious colorectal distension (> 25mmHg) are putative nociceptors to evoke visceral pain (17). In the current study, the proportion of

385

386

387

388

389

390

391

392

393

394

395

396

397

398

399

400

401

402

403

404

405

406

407

408

409

410

411

412

413

HT-muscular afferents in all stretch-sensitive afferents (25.8%) is in agreement with the range of 14-25% as reported by prior studies via single-fiber recordings (17, 49). In summary, the current approach of using graded colorectal distension of luminal shearing allows us to effectively characterize a putative nociceptive (HT-muscular) and three other afferent classes in the lumbosacral DRG.

415

416

417

418

419

420

421

422

423

424

425

426

427

428

429

430

431

432

433

434

435

436

437

438

439

440

441

442

443

444

This is also the first study to reveal the topological distribution of the four classes of DRG neurons in the L6 DRG. It is striking to see that the putative colorectal nociceptors, i.e., HT-muscular afferents are clustered toward the caudal portion of the DRG whereas the other three afferent classes that encode non-noxious stimuli spread out throughout the L6 DRG. We recognize two limitations of the current study in regards to cell distribution. First, approximately 600 - 2400 neurons close to the dorsal lateral surface were monitored for responses to colorectal distention in each DRG, which comprise less than 25% of the total neuron numbers in mouse lumbosacral DRG. Thus, the topological distribution will likely reflect colorectal neurons in superficial layers, which are likely the target of non-invasive DRG neuromodulation with surface electrodes situated outside the dura mater. Second. only VGLUT2-expressing neurons are characterized in this study, which makes up 97% of lumbosacral colorectal afferents from a prior immunostaining study (4) and more than 78% from our current study (Fig. 1). It is unclear regarding the role of the small proportion of VGLUT3- or VGLUT1-expressing colorectal neurons in visceral hyperalgesia which awaits further investigations. A study on the cutaneous mechanical pain suggests that VGLUT3-expressing DRG neurons do not contribute to behavior mechanical hyperalgesia whereas VGLUT3-expressing spinal dorsal horn neurons do (45).

Our findings of clustering of putative colorectal nociceptors in the caudal region of the DRG could have significant implications for the design of DRG neuromodulations that target lumbosacral DRG for managing IBS-related visceral pain. There are several obvious advantages to targeting the DRG. First, the confined location of DRG in inter-vertebral foramina can significantly reduce electrode lead movement due to changes in patient posture (57). Second, DRG are located outside the enclosure of

cerebrospinal fluid, and are less likely to be influenced by patient posture. Third, DRG contain the somata of sensory afferent neurons only, thus permitting selective neuromodulation of the sensory innervation by avoiding the motor efferents. Fourth, afferent sensitization correlates with the pathophysiology of the somata in the DRG, including changes in excitability (28), gene expression (42-44, 58), membrane and cytosol protein levels (27), and glial cell functions (48). Thus, DRG neuromodulation could have a profound therapeutic impact that outlasts the duration of stimulation (46). Thus, outcomes from this study and future studies using optical electrophysiology to characterize colorectal DRG in health and disease will have great impacts on the non-drug management of IBS-related visceral pain via DRG neuromodulation. In particular, the function and topology of colorectal DRG neurons in the context of prolonged visceral pain await further investigations in long-term mouse models of IBS. In summary, we utilized an optical electrophysiology approach to conduct

high-throughput recordings from mouse colorectal afferents in the lumbosacral DRG. Using a high-speed ultra-low noise sCMOS camera and self-developed plug-in program to automatically analyze evoked GCaMP6f transients, we characterized the functional responses of 791 colorectal neurons to graded colorectal distension and luminal shear flow. We also revealed for the first time that high-threshold muscular afferents are clustered in the caudal region of the L6 DRG. Further research using this established optical recording approach is required to reveal changes of topological distributions of DRG neurons in the context of peripheral afferent sensitization in prolonged visceral pain.

468 **REFERENCES**

- 469 1. Beyak MJ. Visceral afferents determinants and modulation of excitability.
- 470 AutonNeurosci 153: 69-78, 2010.
- 471 2. Beyak MJ, Ramji N, Krol KM, Kawaja MD, and Vanner SJ. Two TTX-resistant
- 472 Na+ currents in mouse colonic dorsal root ganglia neurons and their role in
- 473 colitis-induced hyperexcitability. American journal of physiology Gastrointestinal and
- 474 liver physiology 287: G845-G855, 2004.
- 475 3. Brierley SM, Jones RC, 3rd, Gebhart GF, and Blackshaw LA. Splanchnic and
- 476 pelvic mechanosensory afferents signal different qualities of colonic stimuli in mice.
- 477 Gastroenterology 127: 166-178, 2004.
- 478 4. Brumovsky PR, Robinson DR, La JH, Seroogy KB, Lundgren KH, Albers KM,
- 479 Kiyatkin ME, Seal RP, Edwards RH, Watanabe M, Hokfelt T, and Gebhart GF.
- Expression of vesicular glutamate transporters type 1 and 2 in sensory and autonomic
- neurons innervating the mouse colorectum. *JComp Neurol* 519: 3346-3366, 2011.
- 482 5. Chakravarthy K, Nava A, Christo PJ, and Williams K. Review of Recent
- 483 Advances in Peripheral Nerve Stimulation (PNS). Current pain and headache reports
- 484 20: 60, 2016.
- 485 6. Chemla S and Chavane F. Voltage-sensitive dye imaging: Technique review and
- 486 models. Journal of Physiology-Paris 104: 40-50, 2010.
- 7. Chen L, Ilham SJ, and Feng B. Pharmacological Approach for Managing Pain in
- 488 Irritable Bowel Syndrome: A Review Article. Anesthesiology and pain medicine 7:
- 489 e42747, 2017.
- 490 8. Chen TW, Wardill TJ, Sun Y, Pulver SR, Renninger SL, Baohan A, Schreiter
- 491 ER, Kerr RA, Orger MB, Jayaraman V, Looger LL, Svoboda K, and Kim DS.
- 492 Ultrasensitive fluorescent proteins for imaging neuronal activity. *Nature* 499: 295-300.
- 493 2013.
- 494 9. Chisholm KI, Khovanov N, Lopes DM, La Russa F, and McMahon SB. Large
- 495 Scale In Vivo Recording of Sensory Neuron Activity with GCaMP6. eNeuro 5, 2018.
- 496 10. Christianson JA, McIlwrath SL, Koerber HR, and Davis BM. Transient
- 497 receptor potential vanilloid 1-immunopositive neurons in the mouse are more
- 498 prevalent within colon afferents compared to skin and muscle afferents. *Neuroscience*
- 499 140: 247-257, 2006.
- 500 11. Christianson JA, Traub RJ, and Davis BM. Differences in spinal distribution
- and neurochemical phenotype of colonic afferents in mouse and rat. The Journal of
- 502 comparative neurology 494: 246-259, 2006.
- 12. Edelstein AD, Tsuchida MA, Amodaj N, Pinkard H, Vale RD, and Stuurman N.
- 504 Advanced methods of microscope control using μ Manager software. Journal of
- 505 biological methods 1, 2014.
- 13. Emery EC, Luiz AP, Sikandar S, Magnusdottir R, Dong X, and Wood JN. In
- 507 vivo characterization of distinct modality-specific subsets of somatosensory neurons
- 508 using GCaMP. Science advances 2: e1600990, 2016.
- 509 14. Feng B, Brumovsky PR, and Gebhart GF. Differential roles of stretch-sensitive
- 510 pelvic nerve afferents innervating mouse distal colon and rectum. American journal of

- 511 physiology Gastrointestinal and liver physiology 298: G402-409, 2010.
- 512 15. Feng B and Gebhart GF. Characterization of silent afferents in the pelvic and
- 513 splanchnic innervations of the mouse colorectum. American journal of physiology
- Gastrointestinal and liver physiology 300: G170-180, 2011.
- 515 16. Feng B and Gebhart GF. In vitro functional characterization of mouse colorectal
- afferent endings. Journal of visualized experiments: JoVE: 52310, 2015.
- 517 17. Feng B, Joyce SC, and Gebhart GF. Optogenetic activation of mechanically
- 518 insensitive afferents in mouse colorectum reveals chemosensitivity. American journal
- of physiology Gastrointestinal and liver physiology 310: G790-798, 2016.
- 18. Feng B, Kiyatkin ME, La JH, Ge P, Solinga R, Silos-Santiago I, and Gebhart
- 521 **GF.** Activation of guanylate cyclase-C attenuates stretch responses and sensitization
- of mouse colorectal afferents. The Journal of neuroscience : the official journal of the
- 523 Society for Neuroscience 33: 9831-9839, 2013.
- 19. Feng B, La JH, Schwartz ES, and Gebhart GF. Irritable bowel syndrome:
- 525 methods, mechanisms, and pathophysiology. Neural and neuro-immune mechanisms
- of visceral hypersensitivity in irritable bowel syndrome. *American journal of physiology*
- 527 Gastrointestinal and liver physiology 302: G1085-1098, 2012.
- 528 20. Feng B, La JH, Schwartz ES, Tanaka T, McMurray TP, and Gebhart GF.
- 529 Long-term sensitization of mechanosensitive and -insensitive afferents in mice with
- 530 persistent colorectal hypersensitivity. American journal of physiology Gastrointestinal
- 531 and liver physiology 302: G676-683, 2012.
- 532 21. Feng B, La JH, Tanaka T, Schwartz ES, McMurray TP, and Gebhart GF.
- 533 Altered colorectal afferent function associated with TNBS-induced visceral
- 534 hypersensitivity in mice. American journal of physiology Gastrointestinal and liver
- 535 physiology 303: G817-824, 2012.
- 536 22. Feng B, Zhu Y, La JH, Wills ZP, and Gebhart GF. Experimental and
- 537 computational evidence for an essential role of NaV1.6 in spike initiation at
- 538 stretch-sensitive colorectal afferent endings. Journal of neurophysiology 113:
- 539 2618-2634, 2015.
- 540 23. Feng BG, Tiantian; Trocki, Kyle R.; Bian, Zichao; Chen, Longtu; Zheng,
- 541 **Guoan.** Optical electrophysiology reveals topological distribution of functionally
- 542 classified colorectal afferent neurons in intact lumbosacral DRG. 17th WORLD
- 543 CONGRESS ON PAIN, Boston, MA. International Association for the Study of Pain,
- 544 2018.
- 545 24. Foreman RD and Linderoth B. Neural mechanisms of spinal cord stimulation.
- 546 Int Rev Neurobiol 107: 87-119, 2012.
- 547 25. Gemes G, Rigaud M, Koopmeiners AS, Poroli MJ, Zoga V, and Hogan QH.
- 548 Calcium signaling in intact dorsal root ganglia: new observations and the effect of
- 549 injury. Anesthesiology 113: 134-146, 2010.
- 550 26. Ghitani N, Barik A, Szczot M, Thompson JH, Li C, Le Pichon CE, Krashes MJ,
- 551 and Chesler AT. Specialized Mechanosensory Nociceptors Mediating Rapid
- 552 Responses to Hair Pull. *Neuron* 95: 944-954 e944, 2017.
- 553 27. **Gold MS.** Tetrodotoxin-resistant Na+ currents and inflammatory hyperalgesia.
- 554 Proc Natl Acad Sci U S A 96: 7645-7649, 1999.

- 555 28. Gold MS and Flake NM. Inflammation-mediated hyperexcitability of sensory
- 556 neurons. *Neurosignals* 14: 147-157, 2005.
- 557 29. Hibberd TJ, Kestell GR, Kyloh MA, Brookes SJ, Wattchow DA, and Spencer
- NJ. Identification of different functional types of spinal afferent neurons innervating the
- mouse large intestine using a novel CGRPalpha transgenic reporter mouse. *American*
- journal of physiology Gastrointestinal and liver physiology 310: G561-573, 2016.
- 561 30. Hockley JRF, Taylor TS, Callejo G, Wilbrey AL, Gutteridge A, Bach K,
- Winchester WJ, Bulmer DC, McMurray G, and Smith ESJ. Single-cell RNAseq
- reveals seven classes of colonic sensory neuron. *Gut*, 2018.
- 31. **Joseph EK and Levine JD.** Hyperalgesic priming is restricted to isolectin
- 565 B4-positive nociceptors. *Neuroscience* 169: 431-435, 2010.
- 566 32. Kamp EH, Jones RC, III, Tillman SR, and Gebhart GF. Quantitative
- assessment and characterization of visceral nociception and hyperalgesia in mice.
- 568 AmJPhysiol GastrointestLiver Physiol 284: G434-G444, 2003.
- 569 33. Kim YS, Anderson M, Park K, Zheng Q, Agarwal A, Gong C, Saijilafu, Young
- 570 L, He S, LaVinka PC, Zhou F, Bergles D, Hanani M, Guan Y, Spray DC, and Dong
- 571 X. Coupled Activation of Primary Sensory Neurons Contributes to Chronic Pain.
- 572 Neuron 91: 1085-1096, 2016.
- 573 34. Krames ES. The dorsal root ganglion in chronic pain and as a target for
- 574 neuromodulation: a review. Neuromodulation: journal of the International
- 575 Neuromodulation Society 18: 24-32; discussion 32, 2015.
- 576 35. Kyloh M, Nicholas S, Zagorodnyuk VP, Brookes SJ, and Spencer NJ.
- 577 Identification of the visceral pain pathway activated by noxious colorectal distension in
- 578 mice. Front Neurosci 5: 16, 2011.
- 579 36. La JH, Feng B, Kaji K, Schwartz ES, and Gebhart GF. Roles of isolectin
- 580 B4-binding afferents in colorectal mechanical nociception. *Pain* 157: 348-354, 2016.
- 581 37. La JH, Feng B, Schwartz ES, Brumovsky PR, and Gebhart GF. Luminal
- 582 hypertonicity and acidity modulate colorectal afferents and induce persistent visceral
- 583 hypersensitivity. American journal of physiology Gastrointestinal and liver physiology
- 584 303: G802-809, 2012.
- 38. La JH, Schwartz ES, and Gebhart GF. Differences in the expression of transient
- 586 receptor potential channel V1, transient receptor potential channel A1 and
- 587 mechanosensitive two pore-domain K+ channels between the lumbar splanchnic and
- 588 pelvic nerve innervations of mouse urinary bladder and colon. Neuroscience 186:
- 589 179-187, 2011.
- 39. Liem L, van Dongen E, Huygen FJ, Staats P, and Kramer J. The Dorsal Root
- 591 Ganglion as a Therapeutic Target for Chronic Pain. Regional anesthesia and pain
- 592 *medicine* 41: 511-519, 2016.
- 593 40. Malin S, Molliver D, Christianson JA, Schwartz ES, Cornuet P, Albers KM,
- 594 and Davis BM. TRPV1 and TRPA1 function and modulation are target tissue
- 595 dependent. *JNeurosci* 31: 10516-10528, 2011.
- 596 41. Malin SA, Christianson JA, Bielefeldt K, and Davis BM. TPRV1 expression
- 597 defines functionally distinct pelvic colon afferents. The Journal of neuroscience : the
- official journal of the Society for Neuroscience 29: 743-752, 2009.

- 599 42. Miller RJ, Jung H, Bhangoo SK, and White FA. Cytokine and chemokine
- 600 regulation of sensory neuron function. Handbook of experimental pharmacology:
- 601 417-449, 2009.
- 602 43. Obata K and Noguchi K. BDNF in sensory neurons and chronic pain.
- 603 Neuroscience research 55: 1-10, 2006.
- 604 44. Obata K and Noguchi K. MAPK activation in nociceptive neurons and pain
- 605 hypersensitivity. *Life Sci* 74: 2643-2653, 2004.
- 606 45. Peirs C, Williams SP, Zhao X, Walsh CE, Gedeon JY, Cagle NE, Goldring AC,
- 607 Hioki H, Liu Z, Marell PS, and Seal RP. Dorsal Horn Circuits for Persistent
- 608 Mechanical Pain. *Neuron* 87: 797-812, 2015.
- 609 46. Pope JE, Deer TR, and Kramer J. A systematic review: current and future
- 610 directions of dorsal root ganglion therapeutics to treat chronic pain. Pain medicine
- 611 (Malden, Mass) 14: 1477-1496, 2013.
- 612 47. Prato V, Taberner FJ, Hockley JRF, Callejo G, Arcourt A, Tazir B, Hammer L,
- 613 Schad P, Heppenstall PA, Smith ES, and Lechner SG. Functional and Molecular
- 614 Characterization of Mechanoinsensitive "Silent" Nociceptors. Cell reports 21:
- 615 3102-3115, 2017.
- 48. Schaeffer V, Meyer L, Patte-Mensah C, and Mensah-Nyagan AG. Progress in
- 617 dorsal root ganglion neurosteroidogenic activity: basic evidence and
- pathophysiological correlation. *Prog Neurobiol* 92: 33-41, 2010.
- 619 49. Sengupta JN and Gebhart GF. Mechanosensitive afferent fibers in the
- 620 gastrointestinal and lower urinary tracts. In: Visceral Pain, edited by Gebhart GF. Iowa
- 621 City, Iowa: IASP Press, 1995, p. 75-98.
- 50. Smith-Edwards KM, DeBerry JJ, Saloman JL, Davis BM, and Woodbury CJ.
- 623 Profound alteration in cutaneous primary afferent activity produced by inflammatory
- 624 mediators. *eLife* 5, 2016.
- 51. Spencer NJ, Kyloh M, and Duffield M. Identification of different types of spinal
- 626 afferent nerve endings that encode noxious and innocuous stimuli in the large
- intestine using a novel anterograde tracing technique. *PloS one* 9: e112466, 2014.
- 52. Stucky CL and Lewin GR. Isolectin B(4)-positive and -negative nociceptors are
- 629 functionally distinct. *J Neurosci* 19: 6497-6505, 1999.
- 53. Tanaka T, Shinoda M, Feng B, Albers KM, and Gebhart GF. Modulation of
- of the visceral hypersensitivity by glial cell line-derived neurotrophic factor family receptor
- 632 α-3 in colorectal afferents. American journal of physiology Gastrointestinal and
- 633 liver physiology 300: G418-424, 2011.
- 634 54. Verne GN, Robinson ME, Vase L, and Price DD. Reversal of visceral and
- cutaneous hyperalgesia by local rectal anesthesia in irritable bowel syndrome (IBS)
- 636 patients. *Pain* 105: 223-230, 2003.
- 55. **Verne GN, Sen A, and Price DD.** Intrarectal lidocaine is an effective treatment
- for abdominal pain associated with diarrhea-predominant irritable bowel syndrome.
- 639 The journal of pain: official journal of the American Pain Society 6: 493-496, 2005.
- 640 56. Yang X, Li H, and Zhou X. Nuclei Segmentation Using Marker-Controlled
- Watershed, Tracking Using Mean-Shift, and Kalman Filter in Time-Lapse Microscopy.
- 642 IEEE Transactions on Circuits and Systems I: Regular Papers 53: 2405-2414, 2006.

643 57. Zhang TC, Janik JJ, and Grill WM. Mechanisms and models of spinal cord 644 stimulation for the treatment of neuropathic pain. Brain research 1569: 19-31, 2014. 58. Zhang X, Xu ZO, Shi TJ, Landry M, Holmberg K, Ju G, Tong YG, Bao L, 645 Cheng XP, Wiesenfeld-Hallin Z, Lozano A, Dostrovsky J, and Hokfelt T. 646 Regulation of expression of galanin and galanin receptors in dorsal root ganglia and 647 648 spinal cord after axotomy and inflammation. Ann N Y Acad Sci 863: 402-413, 1998. 649 59. Zhu Y, Feng B, Schwartz ES, Gebhart GF, and Prescott SA. Novel method to 650 assess axonal excitability using channelrhodopsin-based photoactivation. Journal of 651 neurophysiology 113: 2242-2249, 2015.

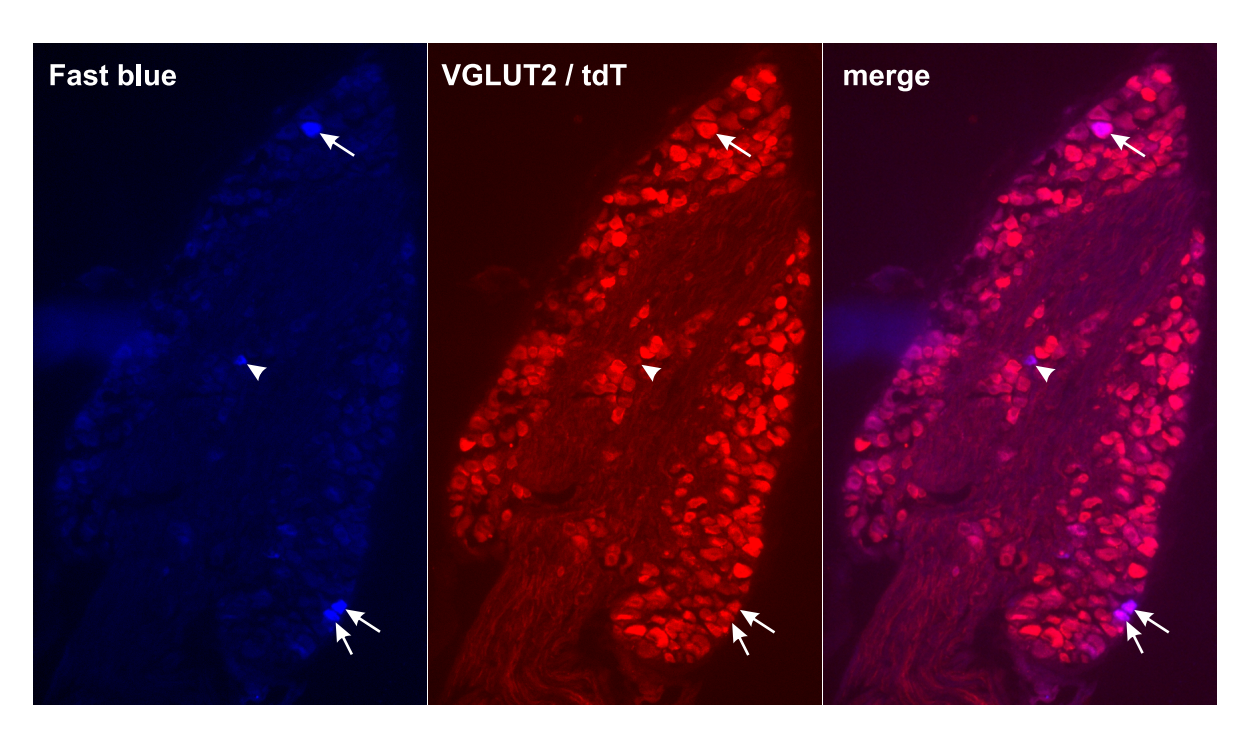
FIGURE LEGENDS

- Fig. 1. VGLUT2-Cre efficiently drives gene expression in colorectal DRG neurons. Neural tracer Fast Blue (FB) injected into the colon wall was retrogradely transported to the lumbosacral DRG as shown in the blue channel. The tdTomato (tdT) expression driven by VGLUT2-Cre was stained by an RFP antibody as shown in the red channel. White arrows indicate colorectal DRG neurons (FB-positive) that are immuno-positive to tdTomato, and white arrowheads indicate colorectal DRG neurons immuno-negative to tdTomato.
- **Fig. 2.** Concurrent GCaMP6f image recording and intracellular sharp electrode recording at L6 DRG. (A) Electrical stimulation was applied to the attached dorsal root via a suction electrode (0.1 ms duration, 1-3 mA) and evoked action potentials were recorded at the DRG both optically by a fluorescent microscope (10x water immersion objective, 0.3 NA) and electrophysiologically by a penetrating sharp quartz glass electrode (100 300 MΩ impedance). A whole DRG can be recorded with a spatial resolution of the GCaMP6f signals at individual DRG neurons (white circle). Optical recordings were conducted at multiple focal planes 50 μm apart to account for the contoured DRG surface. (B)The close correlation of GCaMP6f transients with individual action potentials at 1 Hz stimulation. (C) GCaMP6f signals evoked by electrical stimulations of different frequencies (0.5 8 Hz). (D) Expanded view of the GCaMP6f signals at 4 and 8 Hz stimulation. The GCaMP6f fluorescent signal was normalized by the average intensity and denoted as $\Delta F/F$.
- **Fig. 3.** Functional characterization of colorectal afferents via GCaMP6f DRG recordings in an ex vivo colorectum-pelvic nerve-DRG preparation. (A) The distal colorectum, pelvic nerve and lumbosacral DRG (L5 to S1) were harvested in continuity. The colorectum was cannulated and subjected to two computer-controlled mechanical stimuli: graded colorectal distension (15, 30, 45, 60 mmHg, each for 5 sec) and luminal shear flow (20-30 mL/min). Displayed in (B) and (C) are GCaMP6f recordings of afferent responses to graded colorectal distension and luminal shear flow, respectively.

Fig. 4. Automatic extraction of GCaMP6f transients from image sequences each containing 2700 images by the custom-built plug-in software for Micro-Manager. (A) The boundary of the neurons was automatically determined by marker-based watershed segmentation. (B) Neurons with intensity fluctuation beyond the detection threshold were automatically labeled. (C) GCaMP6f transients extracted from the four labeled neurons in (B).

- **Fig. 5.** Functional classification of 791 lumbosacral colorectal afferents from 8 male and 6 female VGLUT2/GCaMP6f mice. Afferents responding to mechanical colorectal distension or shear flow were predominantly in L6 DRG (90.7%), and also found in S1 (8.3%) and L5 DRG (0.9%). All four afferent classes were present in L6 DRG whereas muscular-mucosal afferents were absent in S1 DRG. LT: low threshold; HT: high threshold. Data from both sexes were pooled together.
- **Fig. 6.** Topological distribution of 718 functionally-classified colorectal afferents in L6 DRG. (A) The GCaMP6f signals were captured from the dorsal lateral view of L6 DRG. (B) Topological distribution of four colorectal afferent classes in L6 DRG: mucosal, LT-muscular, muscular-mucosal and HT-muscular. LT: low threshold; HT: high threshold.

Fig. 1



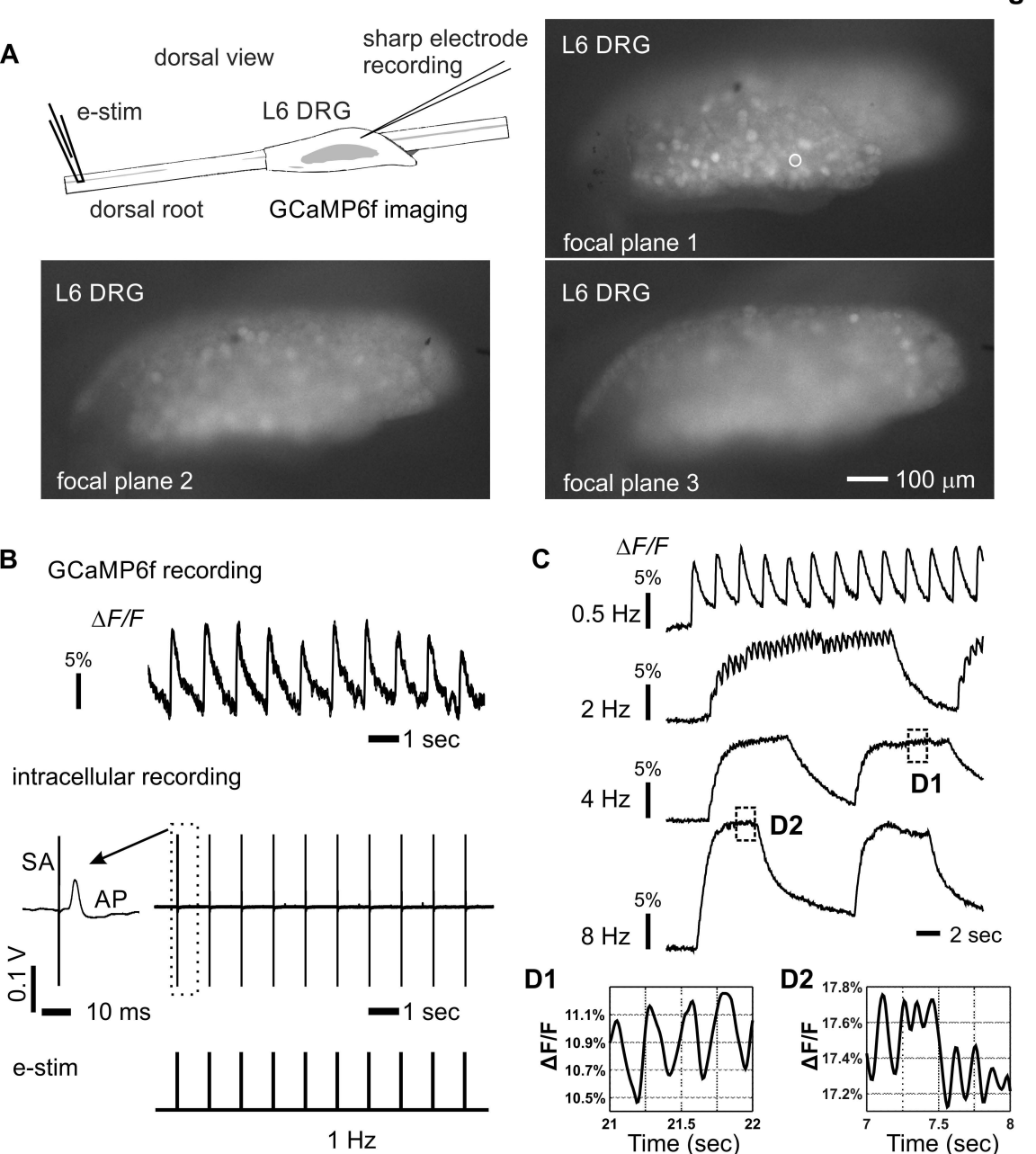
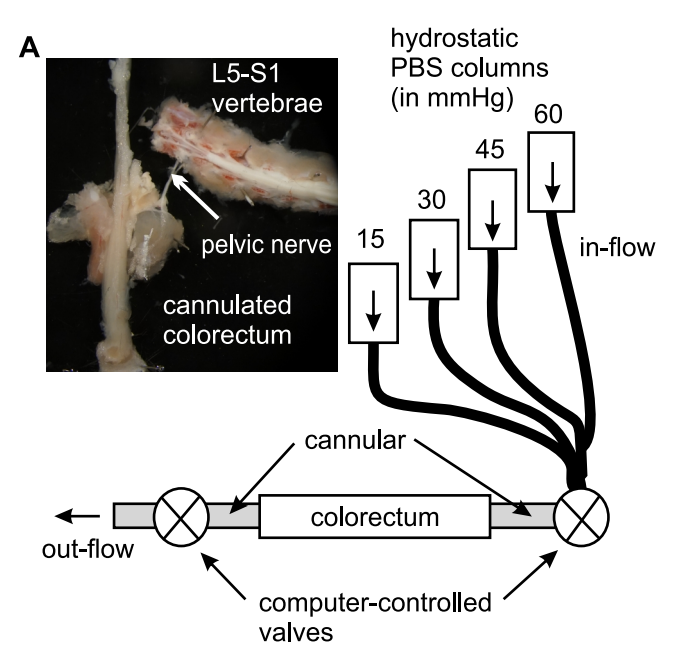
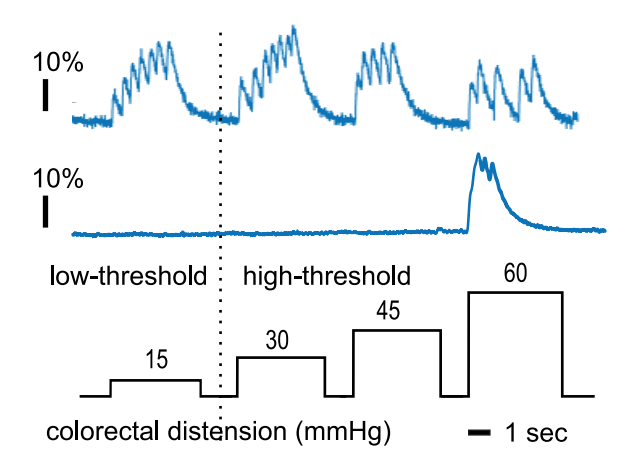


Fig. 3



B normalized GCaMP6 signal from individual DRG



C normalized GCaMP6 signal from individual DRG

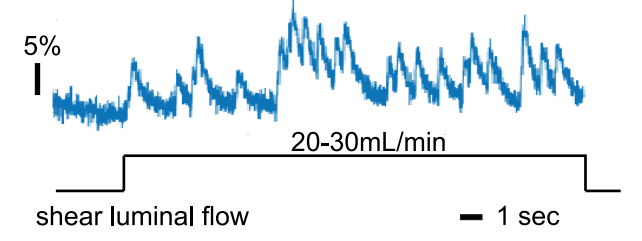


Fig. 4

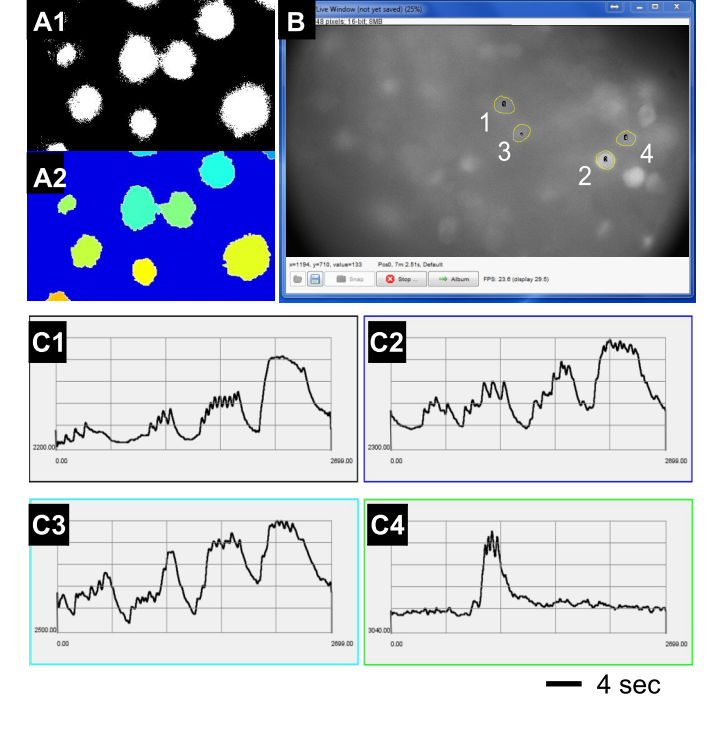


Fig. 5

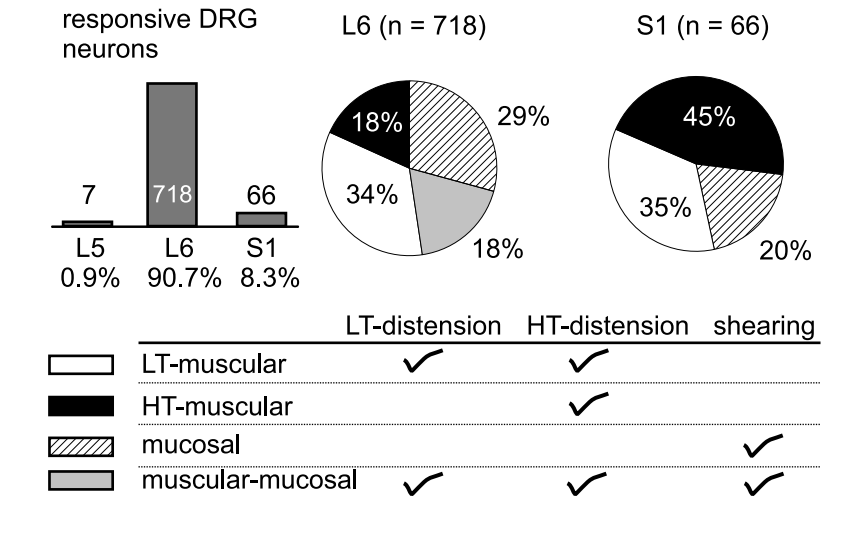


Fig. 6

